DOI: 10.26599/FSHW.2025.9250865

Contents lists available at SciOpen

Food Science and Human Wellness

journal homepage: https://www.sciopen.com/journal/2097-0765

China Food Publishing Co.

Isoliensinine alleviates cardiac apoptosis by activating the PI3K/AKT Pathway: Insights from *in Vivo* and *in Vitro* Studies

Meizhu Wu[1,2,3,4#], Lingqi Chen[1,2,3,4,5#], Zhi Guo[1,2,3,4#], Hongshu Liu[1,2,3,4], Yi Xie[1,2,3,4], Guosheng Lin[1,2,3,4], Qiaoyan Zeng[1,2,3,4], Shilan Chen[1,2,3,4], Rongji Chen[1,2,3,4], Yi Huang[1,2,3,4], Farman Ali[1,2,3,4], Dawei Lian[1,2,3,4], Aling Shen[1,2,3,4]*, Jun Peng[1,2,3,4]*

[1]*Academy of Integrative Medicine, Fujian University of Traditional Chinese Medicine, Fuzhou, Fujian, 350122, China*

[2]*College of Integrative Medicine, Fujian University of Traditional Chinese Medicine, Fuzhou, Fujian, 350122, China*

[3]*Fujian Key Laboratory of Integrative Medicine on Geriatrics, Fujian University of Traditional Chinese Medicine, Fuzhou, Fujian, 350122, China*

[4]*Fujian Collaborative Innovation Center for Integrative Medicine in Prevention and Treatment of Major Chronic Cardiovascular Diseases, Fuzhou, Fujian 350122, China.*

[5]*Overseas Education College, Fujian University of Traditional Chinese Medicine, Fuzhou, Fujian 350122, China.*

ABSTRACT: This study investigated the cardioprotective effects of Isoliensinine, a bisbenzylisoquinoline alkaloid from *Nelumbo nucifera* Gaertn, and its underlying mechanisms. Spontaneous hypertensive rats (SHR) received Isoliensinine (2.5, 5, 10 mg/kg/day) or valsartan (10 mg/kg/day) for 10 weeks, with Wistar-Kyoto rats as controls. Cardiac function, histopathology, apoptosis, and transcriptomic changes were evaluated *in vivo* and in Angtension II (AngII)-stimulated H9c2 cardiomyocytes *in vitro*. Isoliensinine significantly improved left ventricular function, and ameliorated pathological cardiac damage in SHR. Transcriptomic analysis revealed that Isoliensinine reversed 111 up-regulated and 127 down-regulated transcripts in cardiac tissues of SHR, with enrichment of pathways related to apoptosis and the phosphoinositide 3-kinase (PI3K)/protein kinase B (AKT) signaling pathway. Both *in vivo* and *in vitro* experiments confirmed that Isoliensinine reduced cardiomyocyte apoptosis and restored PI3K/AKT phosphorylation. Cellular thermal shift assay (CETSA) and molecular docking supported potential binding of Isoliensinine to PI3K and AKT. Co-treatment with PI3K/AKT activator 740Y-P did not negate the effects of Isoliensinine, suggesting pathway specificity. These findings indicated that Isoliensinine alleviates hypertensive cardiac dysfunction by inhibiting cardiomyocyte apoptosis primarily through modulation of the PI3K/AKT pathway and may serve as a promising therapeutic agent for hypertension.

Keywords: Hypertension, Cardiac injury, Cardiomyocyte apoptosis, Isoliensinine, PI3K/AKT pathway

1. Introduction

Hypertension remains one of the leading risk factors for cardiovascular morbidity and mortality worldwide, contributing to the development of heart failure, arrhythmia, and other cardiac complications[1, 2].

[#]These authors have contributed equally to this work and share first authorship.
***Corresponding author**
saling86@hotmail.com (Aling Shen),
pjunlab@hotmail.com (Jun Peng).

Received 4 April 2025
Received in revised from 31 May 2025
Accepted 27 August 2025

Chronic hypertension induces pathological cardiac remodeling, including cardiomyocyte hypertrophy, apoptosis and fibrosis, which collectively impair cardiac contractile function and lead to irreversible structural damage[3, 4]. Among these, cardiomyocyte apoptosis has been increasingly recognized as a critical factor in hypertensionsive cardiac injury due to the non-renewable nature of cardiomyocytes[5, 6]. Apoptosis, a form of programmed cell death, is initiated by irreversible DNA damage and is distinguished by specific biochemical and morphological alterations[7]. Notably, the apoptosis of cardiomyocytes is pivotal in several physiological processes underlying systolic cardiac dysfunction and the progression to heart failure[8-10]. Targeting apoptosis-related pathways presents a promising therapeutic strategy for mitigating cardiomyocyte apoptosis and preserving cardiac function in hypertensive patients[11, 12].

The mechanisms underlying cardiac injury are intricate and multifaceted, involving a complex interplay of intracellular signaling pathways[13, 14]. Among these pathways, phosphatidylinositol-3-kinase/protein kinase B (PI3K/AKT) signaling pathway plays a role regulator in regulating cell survival and apoptosis in cardiovascular diseases[15-18]. Inhibition of this pathway has been implicated in hypertension-induced cardiomyocyte apoptosis and cardiac dysfunction[19, 20]. Therefore, targeting the PI3K/AKT pathway presents significant therapeutic potential for mitigating cardiac injury and improving cardiovascular outcomes.

Isoliensinine (Iso), a bisbenzylisoquinoline alkaloid derived from the traditional Chinese medicinal plant lotus (*Nelumbo nucifera* Gaertn), possesses diverse pharmacological properties, including anti-inflammatory, antioxidant, and anticancer properties[21-23]. Compared to other natural compounds such as resveratrol and quercetin, Isoliensinine is distinguished by its unique bisbenzylisoquinoline structure, which may underlie its distinct biological effects. Recent studies have suggested that Isoliensinine has therapeutic potential in cardiovascular diseases, particularly through its blood pressure-lowering effects[24]. However, its potential in alleviating hypertension-induced cardiac injury remains largely unexplored. In particular, whether Isoliensinine exerts cardioprotective effects by modulating the PI3K/AKT signaling pathway—a key regulator of cell survival and apoptosis—has not been elucidated.

This study aims to investigate the anti-apoptotic effects of Isoliensinine in a hypertensive setting using Spontaneous hypertensive rats (SHR) and AngII-stimulated H9c2 cells as *in vivo* and *in vitro* models. By employing transcriptomic analysis, functional enrichment studies, and biochemical assays, we sought to elucidate the regulatory mechanisms of Isoliensinine, including the PI3K/AKT pathway. These findings may provide new insights into the therapeutic potential of Isoliensinine for the treatment of hypertensive cardiac injury.

2. Materials and methods

2.1 Reagents

Dulbecco's Modified Eagle Medium (DMEM), Fetal Bovine Serum (FBS), 0.25% Trypsin-EDTA Solution, and the bicinchoninic acid (BCA) Protein Assay Kit were purchased from Thermo Fisher Scientific Inc. (Waltham, MA, USA). The TUNEL apoptosis detection kit (cat. no. C1098) was obtained from Beyotime Biotechnology (Shanghai, China), and the Annexin V-AbFluor™ 647 apoptosis detection kit

(cat. no. 2116) was acquired from Abbkine Scientific Co., Ltd. (Wuhan, Hubei, China). Detailed information regarding the primary and secondary antibodies was provided in Supplementary Table S1. Isoliensinine (cat. no. lianxin-p2) was supplied by Key Pinder Pharm Technology (Shanghai, China).

2.2 Animals

Six 4-week-old male Wistar-Kyoto (WKY) rats and thirty SHR were randomly divided into six groups (n = 6 per group): WKY group, SHR group, SHR + Iso (L) group, SHR + Iso (M) group, SHR + Iso (H) group, and SHR + Valsartan (Val) group. The low, medium, and high-dose Isoliensinine groups were administered Isoliensinine by gavage at doses of 2.5, 5, and 10 mg/kg/day, respectively, while the SHR + Val group received valsartan at a dose of 10 mg/kg/day by gavage. The SHR and WKY groups served as the model and control groups, respectively, and were administered an equivalent volume of double-distilled water by gavage. The experiment lasted for 10 weeks. All experimental animals were purchased from Beijing Vital River Laboratory Animal Technology Co., Ltd. (Beijing, China) and housed at the Laboratory Animal Center of Fujian University of Traditional Chinese Medicine (approval no. 2021189). The animals were maintained in a specific pathogen-free environment with a constant temperature (22–26℃), relative humidity (40%–70%), and a 12 h light/dark cycle. All experimental procedures followed the ethical standards and animal welfare guidelines of the Laboratory Animal Center of Fujian University of Traditional Chinese Medicine under ethical number 2021189.

2.3 Echocardiography

The cardiac contractile function of the rats was assessed using the Vevo 2100 High-Resolution Imaging System (Visual Sonics, Toronto, ON, Canada). The rats were anesthetized with 2% isoflurane for induction and maintained with 1.5% Isoflurane throughout the procedure. A 20-MHz ultrasound probe was utilized to acquire both B-mode and M-mode imaging of the heart. Left ventricular ejection fraction (LVEF), left ventricular fractional shortening (LVFS), interventricular septal thickness at end-diastole (IVS; d), and left ventricular internal diameter at end-diastole (LVID; d) were calculated by using the Vevo software (Visual Sonics; version:3.1.0.13029).

2.4 Hematoxylin and eosin (H&E) staining

Cardiac tissues were fixed with 4% paraformaldehyde for 48 h. The tissues were then dehydrated using a graded ethanol series and embedded in paraffin. Sections were cut at a thickness of 4 μm and deparaffinized using xylene and a graded ethanol series. Hematoxylin staining was performed for 60 sec to label cell nuclei, and eosin staining was applied for 3 sec to label the cytoplasm. Histological analysis and image acquisition were conducted using a Leica intelligent automated optical microscope (Leica Microsystems, Wetzlar, Germany) with a ×400 magnification.

2.5 RNA sequencing analysis

RNA extraction and sequencing of cardiac tissues were performed by CapitalBio Technology (Beijing, China). The samples were rinsed with physiological saline and preserved in RNA stabilization solution prior

to RNA extraction using the TRIzol method. Transcriptome sequencing was carried out on the Illumina platform (Illumina, CA, USA). Differentially expressed transcripts (DETs; n=6) among WKY, SHR, and SHR + Iso (M) groups were identified using DESeq (v1.28.0), and their associated signaling pathways were analyzed using the Kyoto Encyclopedia of Genes and Genomes (KEGG) database. Furthermore, the biological processes (BP), cellular components (CC), and molecular functions (MF) of the DETs were explored through Gene Ontology (GO) analysis.

2.6 RT-qPCR Analysis

Cardiac tissue samples were homogenized in 1 mL of TRIzol reagent (Invitrogen, USA) using grinding beads and a tissue disruptor operating at 50 Hz for five cycles to ensure complete lysis. Following homogenization, 200 μL of chloroform was added, and the samples were shaken vigorously 15 times, then incubated at room temperature for 3 min. The samples were centrifuged at 12,000 × *g* for 15 min at 4℃, and the aqueous phase was carefully collected. An equal volume (500 μL) of isopropanol was added, mixed thoroughly, and incubated at room temperature for 10 min, followed by centrifugation at 12,000 × *g* for 15 mins at 4℃. The resulting RNA pellet was washed with 70% ethanol and centrifuged again at 12,000 × *g* for 10 min at 4℃. After air drying, the RNA pellet was dissolved in RNase-free DEPC-treated water. The RNA concentration and purity were assessed using a NanoDrop spectrophotometer (Thermo Scientific, USA).

Genomic DNA was removed, prior to reverse transcription. Quantitative PCR (qPCR)was then performed according to previously described methods[25]. Forward and reverse primers for *Actb*, *Akt1*, *Atm*, *Ctsh*, *Xiap,* and *GAPDH* are listed in Table 1. *GAPDH* was used as the internal reference gene for normalization of mRNA expression levels.

Table 1. The primers sequence used in RT-qPCR.

Gene	Forward primer (3'→5')	Reveres primer (5'→3')
GAPDH	TATGTCGTGGAGTCTACTGGCG	ATGAGCCCTTCCACGATGC
Actb	CACCATGTACCCAGGCATTG	CCTGCTTGCTGATCCACATC
Akt1	GCCTCTGCTTTGTCATGGAG	AGCATGAGGTTCTCCAGCTT
Atm	AAAGGCAGTGAAGGTTGCTG	AGAGAACCGCGCTAATGAGA
Ctsh	ACAACCAGAGGAACCACACA	GTCCATGGAGGATGGGTAGG
Xiap	CAGCTTGCAAGAGCTGGATT	CTTGGCTTCCAATCCGTGAG

2.7 Terminal deoxynucleotidyl transferase dUTP nick end labeling (TUNEL) staining

Cardiac tissue sections were rehydrated and incubated with 3% H_2O_2 at room temperature for 10 min to block endogenous peroxidase activity. Proteinase K was then applied for antigen retrieval by digestion at 37℃ for 10 min. Subsequently, the sections were incubated with labeling buffer containing TdT and DIG-d-UTP at 37℃ for 2 h. Following this, the sections were treated with a blocking solution for 30 min to minimize nonspecific binding. Biotinylated anti-digoxin antibody and streptavidin-biotin complex solution were applied sequentially, with each incubation performed at 37℃ for 30 min. The sections were treated with 3,3'-diaminobenzidine chromogenic solution for 30 sec, then rinsed with water, lightly counterstained with hematoxylin, dehydrated, and mounted. Finally, the sections were observed and photographed under a Leica intelligent automated optical microscope.

2.8 Cell culture and Isoliensinine treatment

H9c2 cells (rat cardiomyocyte cells, cat. no. CL-0089) were purchased from Procell Life Science & Technology Co., Ltd. (Wuhan, Hubei, China). The cells were cultured in high-glucose DMEM, supplemented with 10% FBS and 1% penicillin-streptomycin in a 37℃ incubator with 5% CO_2. Cells were seeded at a density of 1×10^5 cells/mL and cultured in serum-free DMEM for 4 h. Subsequently, they were treated with Isoliensinine at final concentrations of 2.5, 5, or 10 μmol/L for 48 h, with or without stimulation by AngII (1 μmol/L).

2.9 Annexin-V and propidium iodide (PI) staining

Cells were seeded at 1×10^5 cells/mL density into 6-well plates. After 48 h of treatment with Isoliensinine, with or without stimulation by AngII, the cells were digested with EDTA-free trypsin and collected into flow cytometry tubes. The cells were then resuspended in Annexin V binding buffer and stained with Annexin V-AbFluor™ 647 and PI solution in the dark at room temperature for 30 min. After incubation, 400 μL of Annexin V binding buffer was added to dilute the cell suspension. Flow cytometry analysis was conducted using the BD FACSCanto™ II flow cytometer (BD Biosciences, San Jose, CA, USA). Data were acquired and analyzed using BD FACSDiva™ software (version 8.0).

2.10 Western blotting

Cardiac tissue was first homogenized under liquid nitrogen and then lysed on ice using Western & IP Cell Lysis Buffer (Beyotime Biotech Inc., China) supplemented with a protease inhibitor cocktail, 1 mmol/L phenylmethylsulfonyl fluoride (PMSF), and phosphatase inhibitors. For cultured cells, following drug treatment, cells were harvested using EDTA digestion, collected into centrifuge tubes, and lysed using the same lysis buffer. After lysis, all samples were centrifuged at 12,000 × g for 20 min at 4 ℃ to remove debris. The resulting supernatants were collected, and protein concentrations were determined using a BCA Protein Assay Kit (Beyotime Biotech Inc.). Equal amounts of total protein (50 μg per lane) were separated by 10% SDS-PAGE under a constant voltage of 120 V and transferred onto polyvinylidene fluoride (PVDF) membranes (Millipore, USA) at a constant current of 400 mA. Membranes were blocked with 5% non-fat dry milk in Tris-buffered saline containing 0.1% Tween-20 (TBST) for 2 h at room temperature. After blocking, membranes were washed three times with TBST and incubated overnight at 4 ℃ with primary antibodies diluted in TBST containing 5% bovine serum albumin (BSA). The following day, membranes were incubated with horseradish peroxidase (HRP)-conjugated secondary antibodies (1:5000 dilution) for 1 h at room temperature. Protein bands were visualized using an enhanced chemiluminescence (ECL) detection kit (Beyotime Biotech Inc.), and images were acquired using the Bio-Rad ChemiDoc™ MP Imaging System. Band intensities were quantified using ImageJ software (National Institutes of Health, USA; https://imagej.nih.gov/ij/). *GAPDH* was used as the loading control to normalize protein expression levels.

2.11 Molecular docking

Molecular docking was conducted to analyze Isoliensinine's potential interaction with PI3K and AKT. The 3D structure of Isoliensinine was retrieved from the PubChem database, while the protein structures of PI3K (UniProt ID:P27986; PDB ID:1H9O) and AKT (UniProt ID:P31749; PDB ID:1UNP) were obtained from the RCSB PDB database. Docking simulations were performed using AutoDock Vina, with binding site identification facilitated by AutoDock Tools[26]. Ligands underwent energy minimization using the Avogadro program, and docking exhaustiveness was set to 100. Optimized conformations were visualized and analyzed using Biovia Discovery Studio software, providing detailed insights into the molecular interactions.

2.12 Cellular thermal shift assay

The binding of Isoliensinine with potential protein targets was validated using cellular thermal shift assays (CESTA)[27]. H9c2 cells were lysed on ice for 30 min, and total protein was extracted. Equal amounts of protein (2 mg/mL, 1 mL) were incubated with Isoliensinine (10 μmol/L) or DMSO at room temperature for 1 h. The mixtures were then aliquoted into seven PCR tubes and subjected to heat treatment at seven different temperatures for 5 min each. Subsequently, the samples were cooled on ice for 5 min. After centrifugation at 12,000 × *g* for 20 min, the supernatants were mixed with 5× loading buffer, heated at 95℃ for 5 min, and then used for Western blotting.

2.13 Statistical analysis

Statistical analysis was performed using SPSS 26.0 software (SPSS/PC+, version 23.0, Chicago, IL, USA). For comparisons between two groups, Student's t-test was used for normally distributed data, while the Mann–Whitney U test was applied for non-normal data distribution. For comparisons among multiple groups, the Shapiro-Wilk test was first used to assess data normality. If the data followed a normal distribution with homogeneity of variance, one-way analysis of variance (ANOVA) was performed, followed by post hoc pairwise comparisons using the least significant difference (LSD) test. If the data were normally distributed but exhibited heterogeneity of variance, the Games–Howell test was used for post hoc comparisons. For non-normal distribution data, the Kruskal–Wallis test was employed to evaluate group differences. Data were expressed as the mean ± standard deviation (SD) for normally distributed data. A two-sided P value < 0.05 was considered statistically significant. All experiments were independently repeated at least three times.

3. Results

3.1 Isoliensinine treatment attenuates cardiac dysfunction and morphological changes in SHR

Determination of cardiac function revealed that SHR exhibited decreased LVEF, LVFS and increased IVS; d, and LVID; d, compared to WKY rats. These abnormalities were reversed after Isoliensinine or valsartan treatment (Figure 1A-E). Furthermore, histological examination of cardiac tissue in SHR revealed marked pathological alterations, including disorganized cardiomyocyte arrangement, loss of typical parallel alignment, irregular and crisscrossing myocardial fibers, increased nuclear atypia, widened interstitial spaces,

myocardial bundle fragmentation, and overall structural disarray. In contrast, treatment with Isoliensinine at various doses or with valsartan effectively preserved myocardial architecture, as evidenced by restoration of cardiomyocyte alignment, reduced nuclear abnormalities, and improved interstitial tissue integrity (Figure 1F).

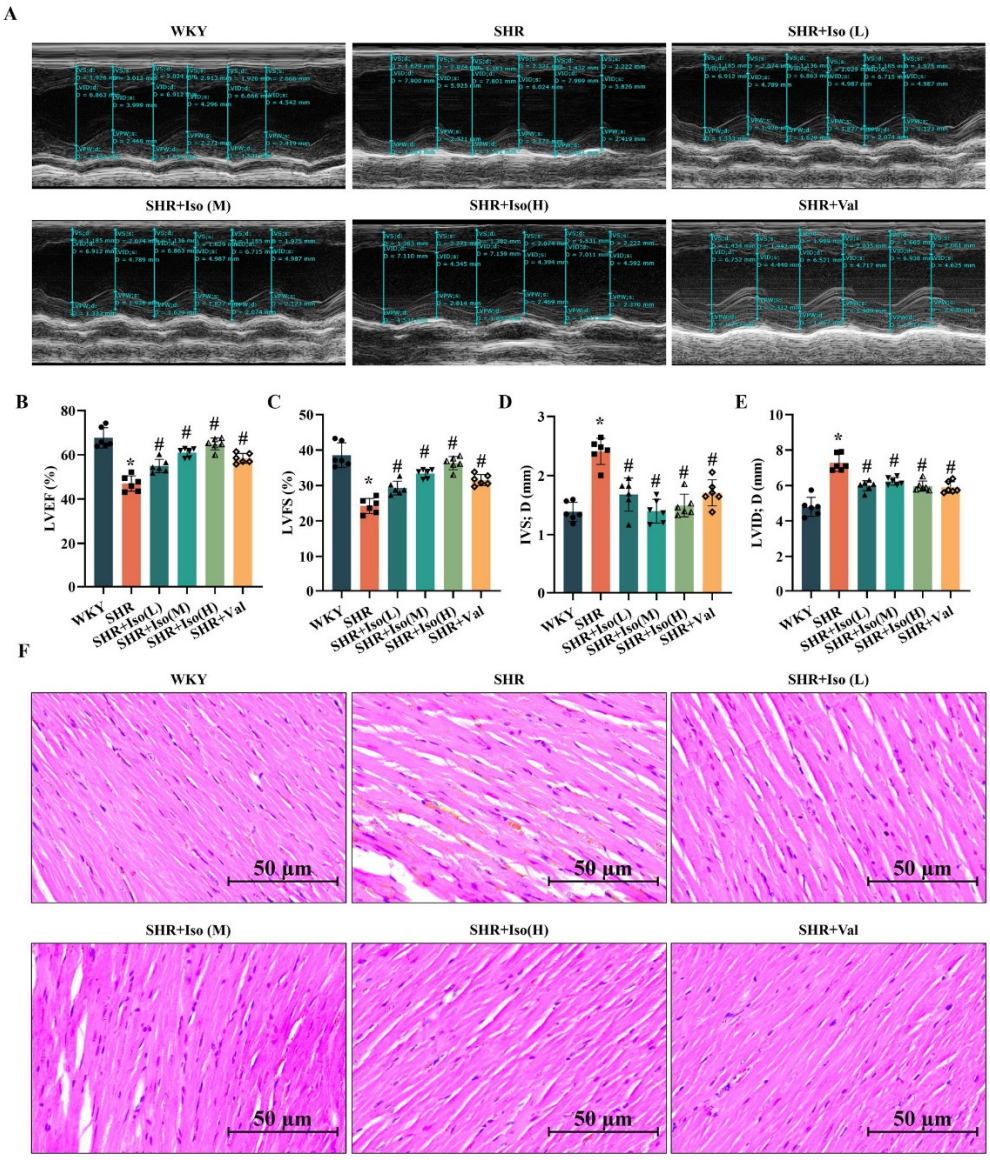

Figure 1. Effects of Isoliensinine treatment on cardiac function and pathological morphological changes in Spontaneously Hypertensive Rats (SHRs).

(A) Representative images of echocardiography from each group of rats. Ultrasound was performed to evaluate the (B) left ventricular ejection fraction (LVEF), (C) left ventricular fractional shortening (LVFS), (D) interventricular septal thickness at end-diastole (IVS; d) and (E) left ventricular internal diameter at end-diastole (LVID; d). (F) Morphological changes in rat cardiac tissues were further analyzed using hematoxylin-eosin (H&E) staining, with images captured at a scale bar of 50 μm under a ×40 objective lens using an optical microscope. Data are presented as mean ± standard deviation. *P < 0.05 vs. WKY group; #P < 0.05 vs. SHR group.

3.2 Effects of Isoliensinine treatment on gene expression in cardiac tissue of SHR

All three groups exhibited substantial intra-group homogeneity in gene expression levels, with red indicating high-expression genes and blue denoting low-expression genes (Figure 2A-B). A total of 2,682 DETs were identified in the cardiac tissue of SHR compared to WKY rats, including 1,335 up-regulated DETs (red) and 1,347 down-regulated DETs (blue) (Figure 2C). In the SHR + Iso (M) group compared to

SHR, a total of 1,096 transcripts were altered, including 526 up-regulated and 568 down-regulated transcripts (Figure 2D). In the comparative analysis between SHR vs. WKY and SHR + Iso (M) vs. SHR, of the 1,347 down-regulated transcripts in SHR vs. WKY, 111 were up-regulated after Isoliensinine treatment (Figure 2E, F). Conversely, of the 1,335 up-regulated transcripts in SHR vs. WKY, 127 were down-regulated after Isoliensinine treatment.

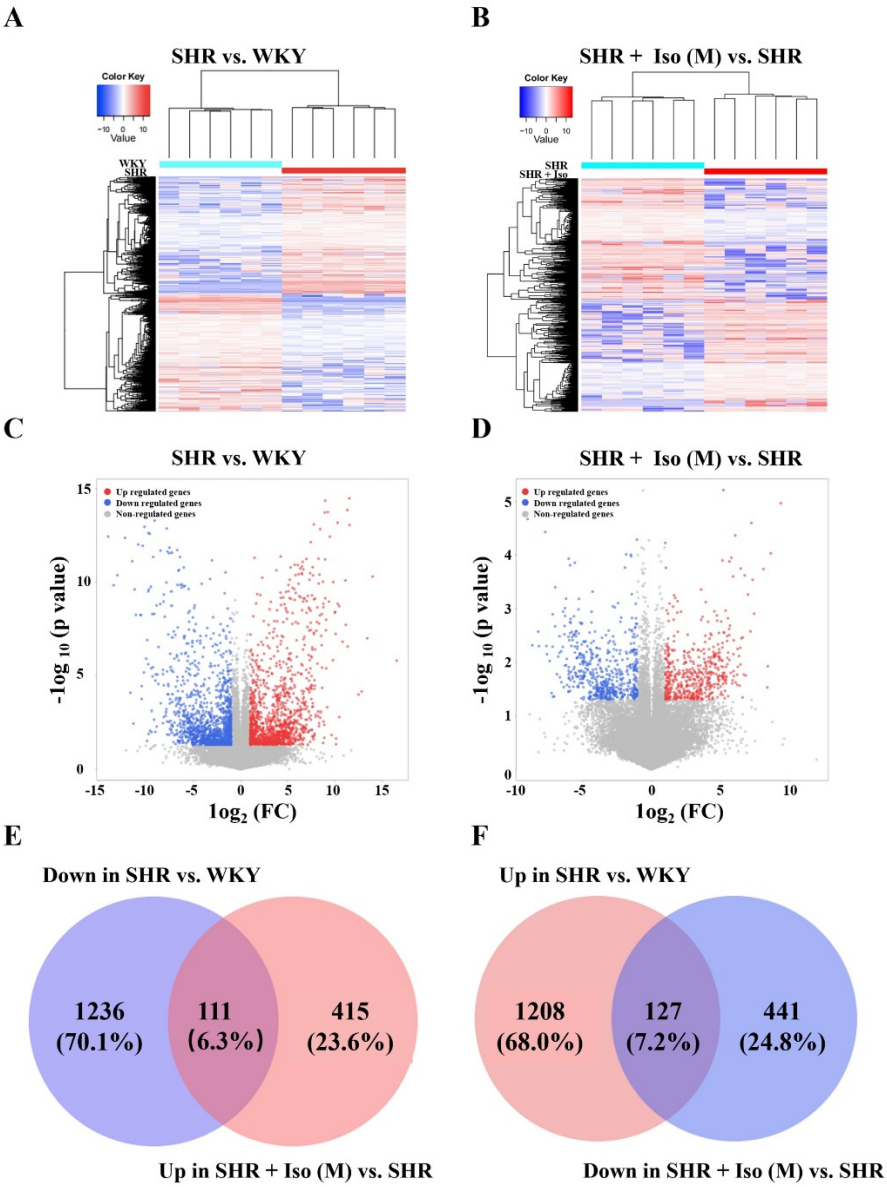

Figure 2. Effects of Isoliensinine treatment on gene expression in cardiac tissue of SHRs.
RNA sequencing was conducted to identify and visualize changes in gene expression within rat cardiac tissues. Differential gene expression was assessed and represented through various analytical approaches: Cluster analysis of gene expression profiles comparing (A) SHR vs. WKY, and (B) SHR + Iso (M) vs. WKY groups (n=6), showcasing distinct expression patterns. Volcano plots illustrating the distribution of significantly differentially expressed transcripts between (C) SHR vs. WKY and (D) SHR + Iso (M) vs. SHR groups (n=6), highlighting upregulated (red) and downregulated (blue) genes. (E, F) Venn diagrams illustrating overlapping differentially expressed transcripts between the comparisons of SHR vs. WKY and SHR + Iso (M) vs. SHR, highlighting the shared differentially expressed genes.

3.3 Effect of Isoliensinine treatment on the bioinformatic characteristics of DETs in cardiac tissue of SHR

Based on the above DETs, a total of 494 BP terms were enriched in comparison of SHR vs. WKY, and 669 BP terms were enriched in comparison of SHR + Iso (M) vs. SHR (Figure 3A). Among these, 100 BP

terms were commonly enriched between the two comparisons, primarily including the regulation of cysteine-type endopeptidase activity involved in the apoptotic process, positive regulation of the apoptotic process, and positive regulation of programmed cell death (Figure 3B). In the CC analysis, 57 CC terms were enriched in comparison of SHR vs. WKY, and 48 CC terms were enriched in comparison of SHR + Iso (M) vs. SHR. Notably, 9 CC terms were commonly enriched between the two comparisons, primarily including cytoplasm, intracellular, and cytosol (Figure 3C, D). 188 MF terms were enriched in comparison of SHR vs. WKY, and 142 MF terms were enriched in comparison of SHR + Iso (M) vs. SHR (Figure 3E). A total of 26 MF terms were commonly enriched, including protein binding, enzyme binding, and small molecule binding (Figure 3F).

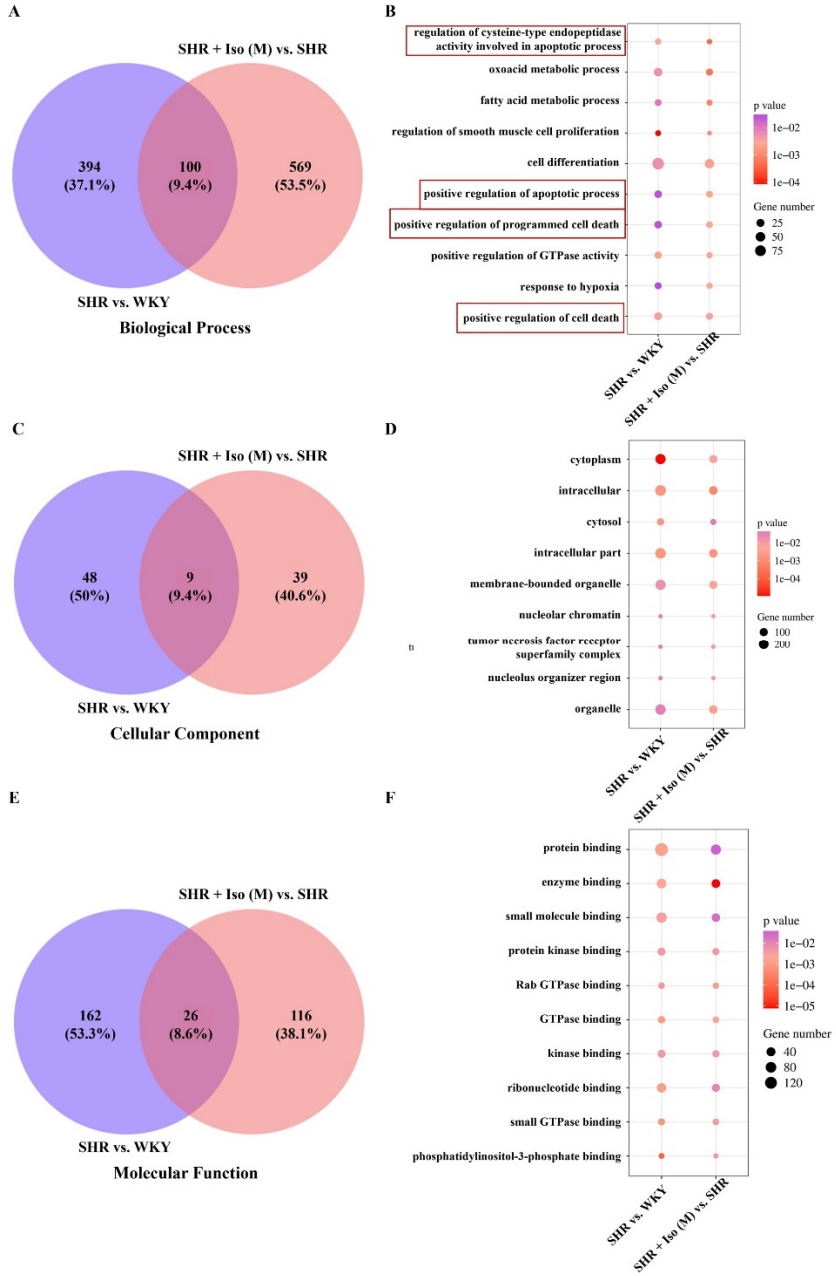

Figure 3. Effects of Isoliensinine treatment on bioinformatic characteristics based on differentially expressed transcripts (DETs) in cardiac tissue of SHRs.

The bioinformatic characteristics of DETs (n=6) in cardiac tissues were analyzed using Gene Ontology (GO) enrichment to identify commonly enriched features in the SHR vs. WKY and SHR + Iso (M) vs. SHR groups. Key shared GO categories were identified, including: (A, B) Biological processes. (C, D) Cellular components. (E, F) Molecular functions.

3.4 Isoliensinine treatment modulates apoptosis pathways in cardiac tissue of SHR

KEGG analysis identified the enrichment of 31 pathways in comparsion of SHR vs. WKY, including viral myocarditis, metabolic pathways, and lysosome (Figure 4A). On the other hand, 16 pathways were significantly enriched in comparison of SHR + Iso (M) vs. SHR, including apoptosis, HIF-1 signaling pathway, mTOR signaling pathway, and lysosome (Figure 4B). A further sub-classification of the KEGG pathways revealed that the primary regulatory pathways affected by Isoliensinine were predominantly associated with apoptosis and lysosome within the cellular processes cluster (Figure 4C). Genes such as *Akt1*, *Atm*, and *Slc1la2* were identified as closely involved in these pathways (Figure 4D). In the analysis of the apoptosis pathway, Isoliensinine may exert its anti-apoptotic apoptosis effects on cardiomyocytes by mediating the activation of the PI3K/AKT pathway through the regulation of AKT1 protein expression or activity (Figure 4E). Within this pathway, five target genes were differentially expressed, including *Actb*, *Akt1*, *Atm*, *Ctsh*, and *Xiap*. To further validate these transcriptomic findings, we performed RT-qPCR to assess the mRNA expression levels of these genes in cardiac tissues from the WKY, SHR, and SHR + Iso (M, 5 mg/kg/day) groups. Compared to the WKY group, the SHR group exhibited increased expression of *Actb* and *Ctsh*, and decreased expression of *Akt1*, *Atm*, and *Xiap* in cardiac tissues. Notably, Isoliensinine treatment reversed these changes, with downregulation of *Actb* and *Ctsh*, and upregulation of *Akt1*, *Atm*, and *Xiap* in cardiac tissues (Figure 4F).

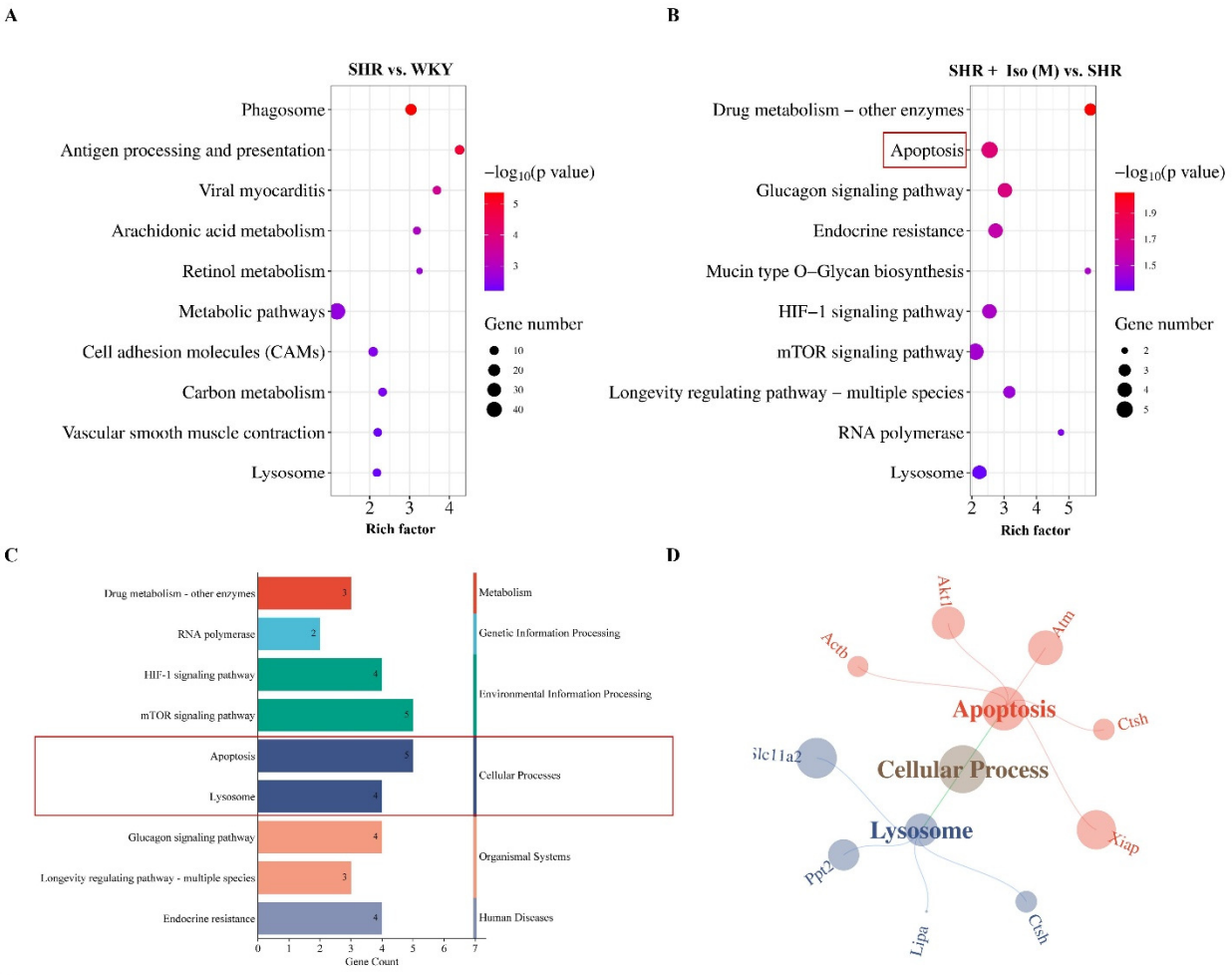

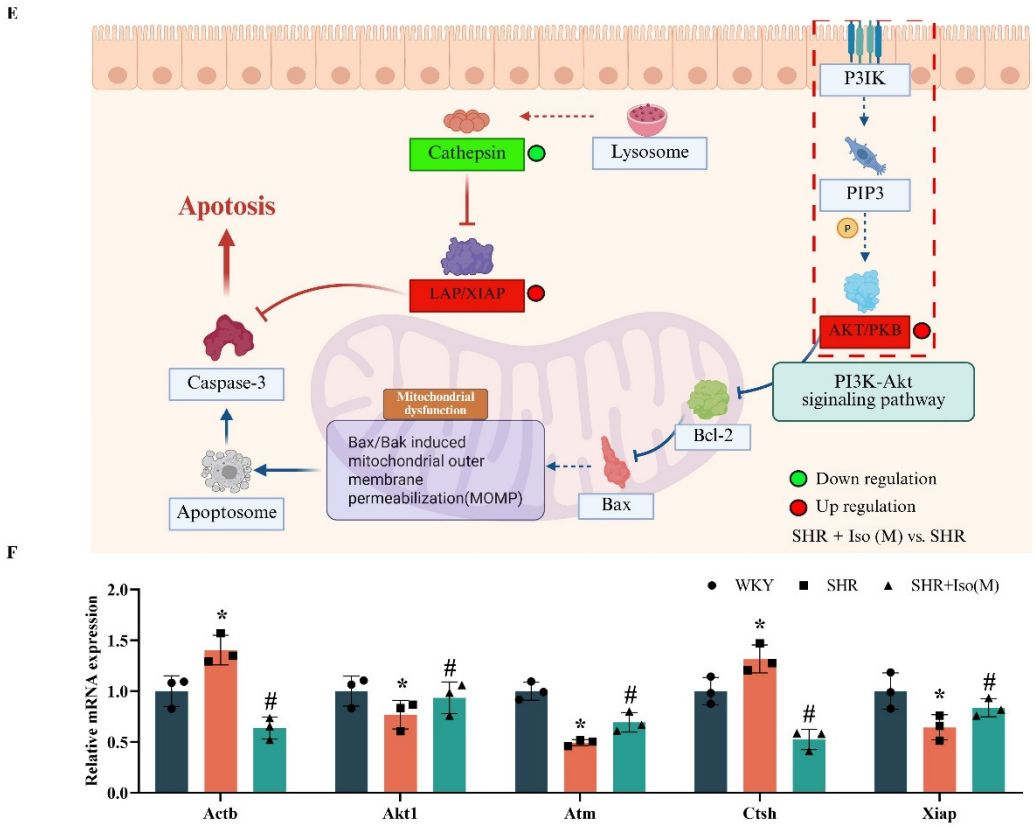

Figure 4. Potential pathways modulated by Isoliensinine treatment based on DETs in cardiac tissue of SHRs. Pathway enrichment analysis of DETs (n=6) was performed using the KEGG database to explore the molecular pathways regulated by Isoliensinine: (A) Pathway enrichment in SHR vs. WKY and (B) SHR + Iso (M) vs. SHR groups, identifying significant pathways influenced by ISO treatment. (C) Secondary classification of enriched pathways was conducted using bioinformatics tools, providing a refined categorization of regulatory pathways. (D) A combined pathway-gene alteration map focused on the Cellular Process category, illustrating the association between specific pathways and corresponding gene changes. (E) A comprehensive regulation diagram depicting the impact of Isoliensinine on the Apoptosis pathway, highlighting its modulatory role in apoptosis-related molecular processes. (F) RT-qPCR analysis of *Actb*, *Akt1*, *Atm*, *Ctsh*, and *Xiap* mRNA expression levels in cardiac tissues from different experimental groups. Data are presented as mean ± standard deviation. Data are presented as mean ± standard deviation. **P* < 0.05 vs. WKY group; #*P* < 0.05 vs. SHR group.

3.5 Isoliensinine treatment reduced cell apoptosis in cardiac tissue of SHR

TUNEL staining revealed that the percentage of TUNEL positively stained cells in cardiac tissues of SHR was significantly increased, which were significantly substantially reduced after Isoliensinine treatment (Figure 5A, B). Western blot analysis revealed that the expression of pro-apoptotic proteins Bax and cleaved caspase-3 were significantly increased and the expression of anti-apoptotic protein Bcl-2 was decreased in cardiac tissues of SHR, which were all reversed after Isoliensinine treatment (Figure 5C-G). These findings suggest that Isoliensinine treatment can significantly inhibit cell apoptosis in the cardiac tissue of SHR.

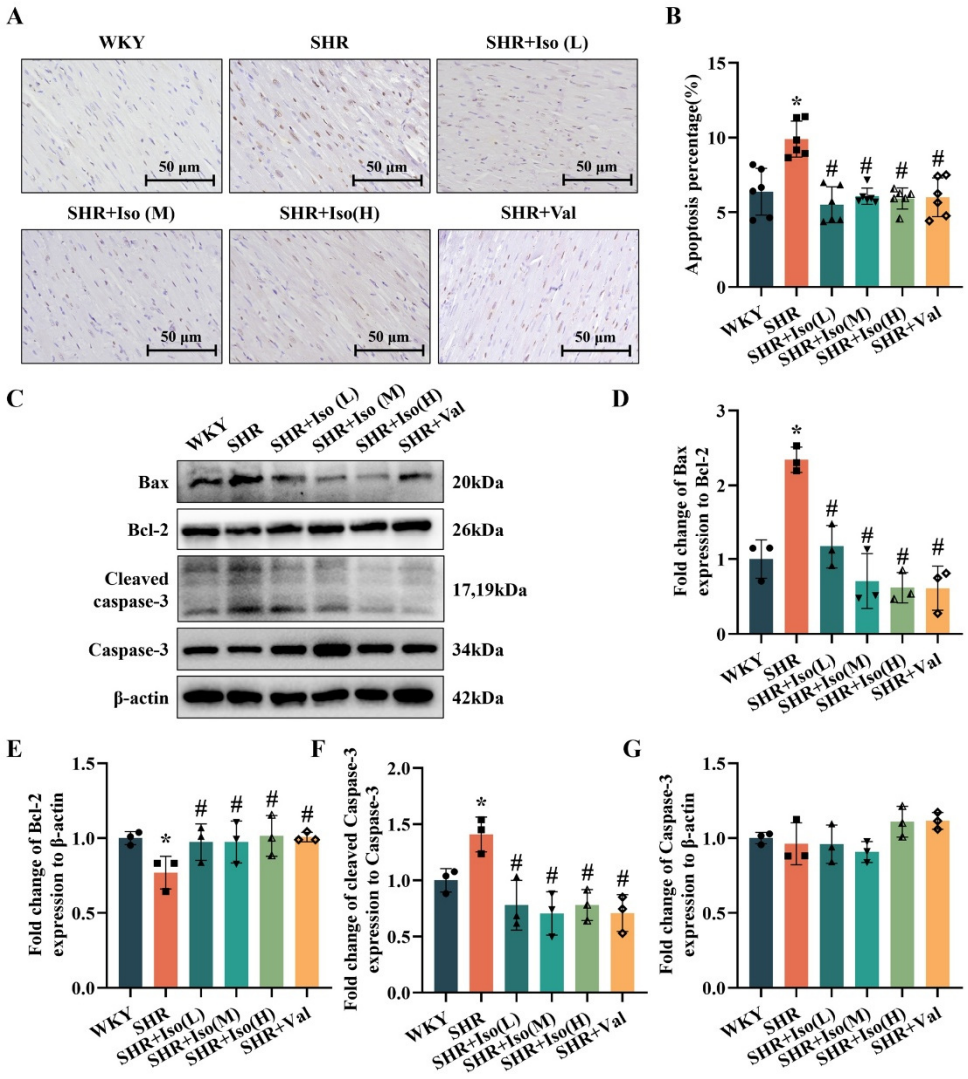

Figure 5. Effects of Isoliensinine treatment on cell apoptosis in the cardiac tissue of SHRs. (A, B) TUNEL staining was used to evaluate the effect of Isoliensinine treatment on apoptosis in rat cardiac tissue. Representative images of apoptotic cells in each group were captured, with a scale bar of 50 μm, using an optical microscope under ×40 objective magnification. (C-G) Western blot analysis was performed to determine the expression levels of key apoptotic markers, including the pro-apoptotic protein Bax, anti-apoptotic protein Bcl-2, and the ratio of cleaved caspase-3 to total caspase-3. Data are presented as mean ± standard deviation. Data are presented as mean ± standard deviation. *$P < 0.05$ vs. WKY group; #$P < 0.05$ vs. SHR group.

3.6 Isoliensinine treatment restores PI3K/AKT pathway activity in vivo

To further explore the molecular underlying mechanism, the PI3K/AKT signaling pathway was explored. Western blot analysis revealed that SHR exhibited significantly decreased the ratio of p-PI3K/PI3K and p-AKT/AKT, which were all increased after Isoliensinine treatment (Figure 6A-E). These findings suggest that Isoliensinine treatment can effectively activate the PI3K/AKT pathway in the cardiac tissue of SHR.

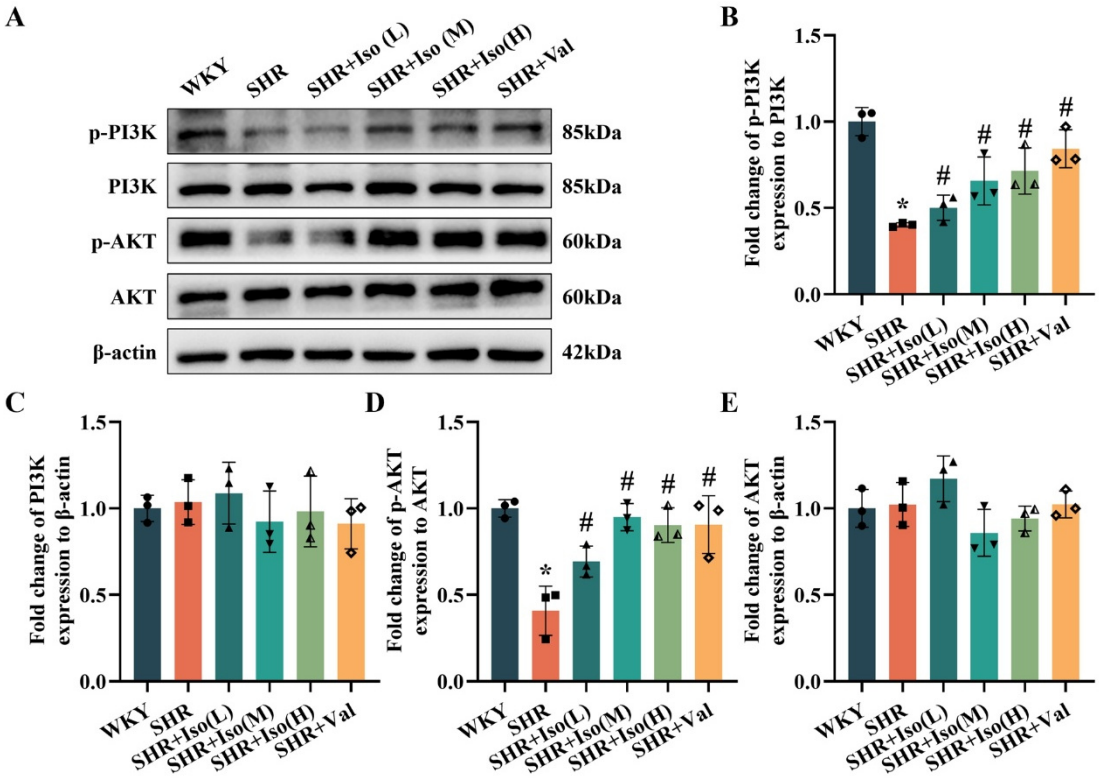

Figure 6. Effects of Isoliensinine treatment on PI3K/AKT pathway activity *in vivo*.
(A) Western blot analysis was performed to evaluate the expression levels of phosphorylated PI3K (p-PI3K), total PI3K, phosphorylated AKT (p-AKT), and total AKT proteins in rat cardiac tissues. (C-E) The relative ratios of p-PI3K/PI3K and p-AKT/AKT were quantified to assess the regulatory effects of Isoliensinine on the PI3K/AKT signaling pathway. Data are expressed as mean ± standard deviation. **P* < 0.05 vs. WKY group; #*P* < 0.05 vs. SHR group.

3.7 Isoliensinine treatment reduced AngII-induced cell apoptosis in H9c2 cells

Annexin V/PI staining showed that AngII simulation increased the rate of apoptosis in H9c2 cells, which were alleviated after different concentrations of Isoliensinine treatment (Figure 7A-B). Consistently, Isoliensinine treatment significantly decreased in the pro-apoptotic proteins Bax and cleaved caspase-3, increased in the anti-apoptotic protein Bcl-2 in AngII-induced H9c2 cells (Figure 7C-H). These findings suggest that Isoliensinine treatment significantly inhibits AngII-induced apoptosis in H9c2 cells.

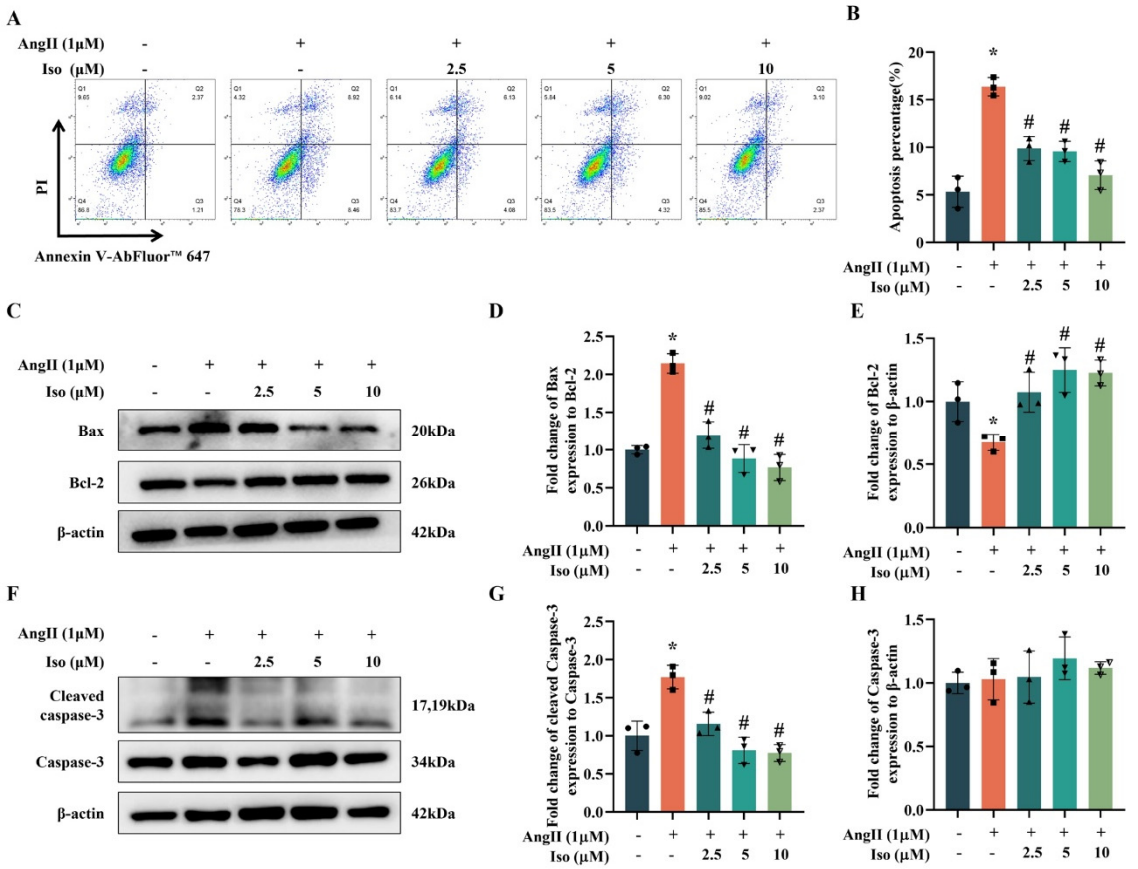

Figure 7. Effects of Isoliensinine treatment on AngII-induced apoptosis in H9c2 cells.

(A) Annexin-V and propidium iodide staining were performed to evaluate the effect of Isoliensinine on cardiomyocyte apoptosis in AngII-induced H9c2 cells, with representative images depicting apoptotic and necrotic cell populations. (B) Quantitative analysis of apoptosis levels demonstrated the significant protective effect of Isoliensinine against AngII-induced cell apoptosis. (C-H) Western blot analysis was conducted to measure the expression levels of pro-apoptotic protein Bax, anti-apoptotic protein Bcl-2, cleaved caspase-3, and total caspase-3 in AngII-induced H9c2 cells after Isoliensinine treatment. Data are presented as mean ± standard deviation, with statistical significance indicated as *$P < 0.05$ vs. the control group; #$P < 0.05$ vs. the AngII group.

3.8 Isoliensinine treatment restores PI3K/AKT pathway activity in vitro

Western blot analysis indicated that ratio of p-PI3K/PI3K and p-AKT/AKT in AngII-stimulated H9C2 cells were significantly decreased, which were all increased after Isoliensinine treatment and didn't affect the total expression of PI3K and AKT (Figure 8A-F). To further investigate whether the PI3K/AKT pathway mediates the anti-apoptotic effect of Isoliensinine on cardiomyocytes, we used a specific activator of the PI3K/AKT pathway. Either 740Y-P (a PI3K/AKT pathway activator) or Isoliensine treatment significantly alleviated AngII-induced apoptosis in H9c2 cells, while combination treatment with 740Y-P and Isoliensine didn't further reduce the apoptosis rate (compared with 740Y-P treatment alone) in AngII stimulated H9c2 cells (Figure 8G, H). These results suggested that Isoliensinine primarily exerts its anti-apoptotic effect through the regulation of the PI3K/AKT pathway (Figure 8G, H).

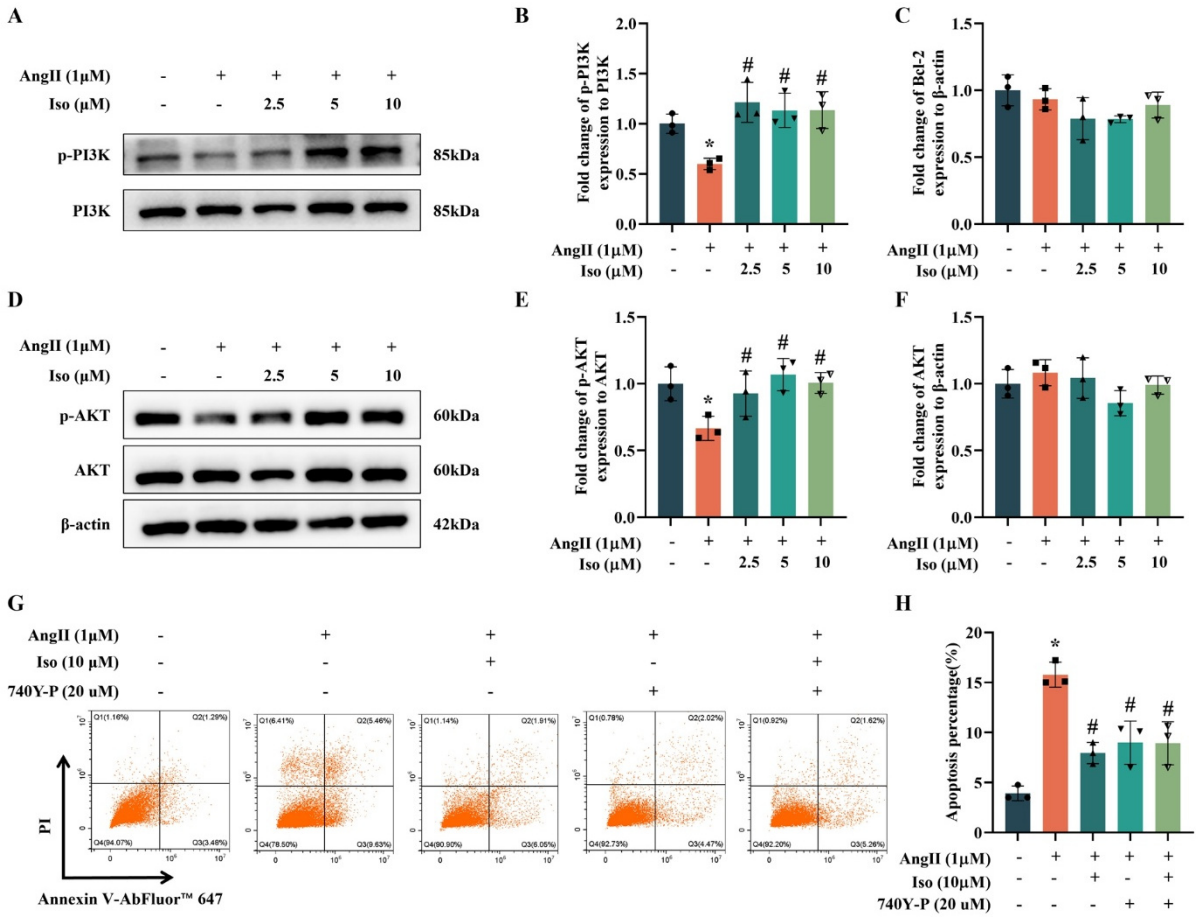

Figure 8. Effects of Isoliensinine treatment on PI3K/AKT pathway activity *in vitro*.
(A-F) Western blot analysis assessed the expression levels of p-PI3K, PI3K, p-AKT, and AKT proteins in AngII-induced H9c2 cells. Quantitative analysis of the protein expression levels revealed that Isoliensinine significantly mitigated AngII-induced dysregulation of the PI3K/AKT signaling pathway, demonstrating its protective effect against AngII-induced cell apoptosis. (G, H) Annexin V and PI staining was conducted to evaluate the effect of Isoliensinine on the PI3K/AKT pathway in AngII-induced H9c2 cells, using the PI3K/AKT pathway activator 740Y-P (20 μmol/L). The data are presented as mean ± standard deviation. **P* < 0.05 vs. the Control group, #*P* < 0.05 vs. the AngII group.

3.9 Isoliensinine potential targets PI3K/AKT pathway to modulate its abnormal inhibition

A CETSA was used to assess the potential interaction between Isoliensinine and the PI3K and AKT proteins. PI3K and AKT exhibited significant thermal stabilization after Isoliensinine treatment, indicating a potential direct binding interaction (Figure 9A, B). To further investigate the binding affinity, molecular docking simulations were performed to explore the interactions between Isoliensinine and PI3K/AKT. The docking results revealed lower binding energy values for Isoliensinine with PI3K (UniProt ID: P27986; PDB ID:1H9O; Binding energy: -5.93 kcal/mol) and AKT (UniProt ID: P31749; PDB ID:1UNP; Binding energy: -5.71 kcal/mol), indicative of strong binding affinities (Figure 9C, D). These findings suggest that Isoliensinine potentially bind to PI3K and AKT.

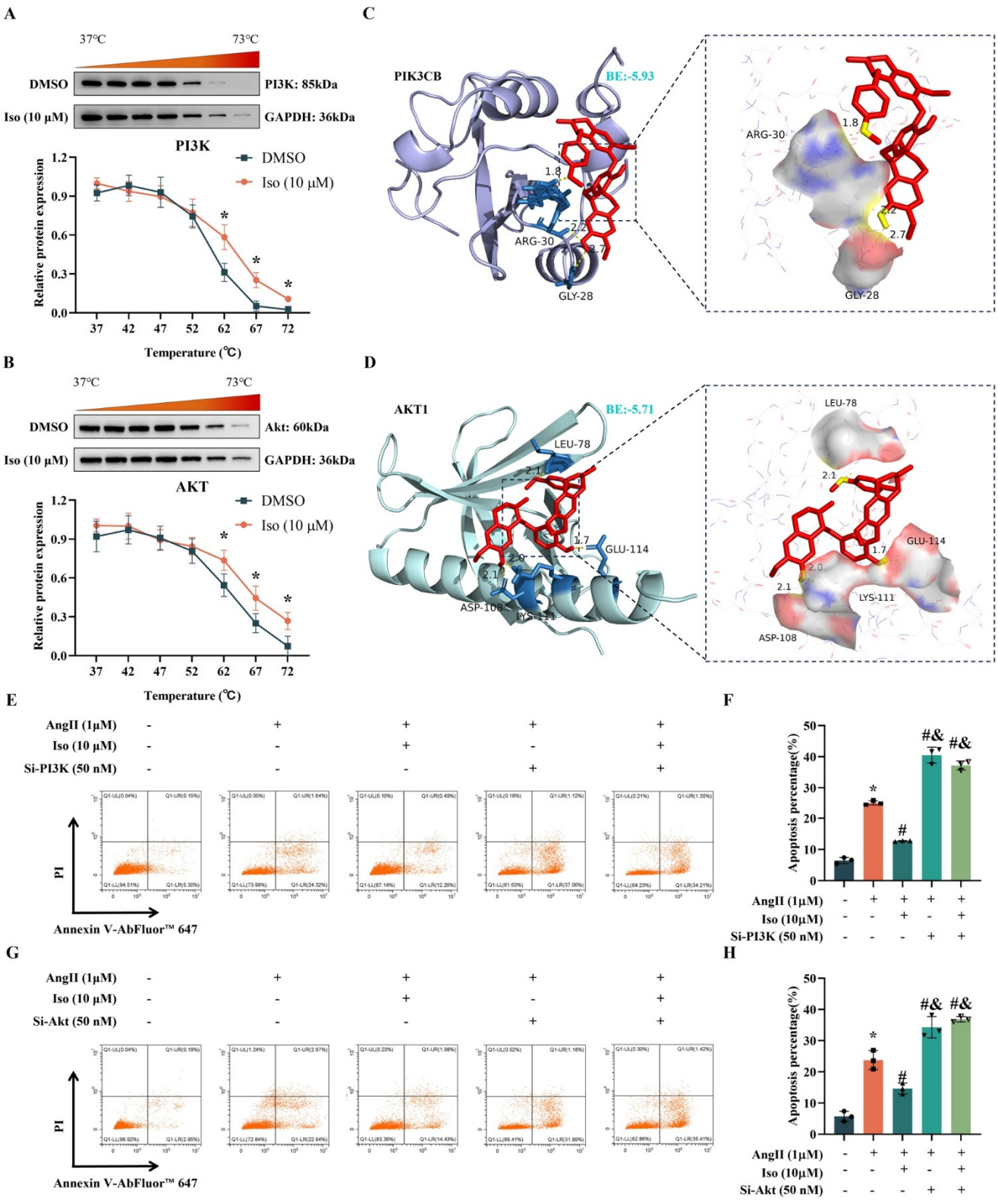

Figure 9. The potential interaction of Isoliensinine with PI3K and AKT.

(A, B) Cellular thermal shift assay (CETSA) combined with Western blotting were performed to evaluate the direct interaction between Isoliensinine and PI3K/AKT in H9c2 cells. Protein extracts from cells treated with Isoliensinine (10 μmol/L) or DMSO were subjected to thermal shift assays, followed by the quantification of soluble proteins. (C, D) Molecular docking simulations were conducted to assess the binding affinity of Isoliensinine to PI3K (UniProt ID: P27986; PDB ID: 1H9O) and AKT (UniProt ID: P31749; PDB ID: 1UNP). (E–H) Annexin V staining was used to assess the impact of PI3K or AKT silencing on the anti-apoptotic effects of Isoliensinine in H9c2 cells. *P < 0.05 vs. the Control group, #P < 0.05 vs. the AngII group; &P < 0.05 vs. the AngII + Iso group.

To further investigate whether PI3K/AKT signaling is a key pathway through which Isoliensinine exerts its anti-apoptotic effects, we conducted additional validation experiments using Annexin V staining assays combined with gene silencing. The results demonstrated that AngII stimulation significantly increased apoptosis in H9C2 cells (Figure 9E-H), which was notably reduced after Isoliensinine treatment. However, silencing of PI3K or AKT (via Si-PI3K or Si-AKT) aggravated AngII-induced apoptosis. Importantly, co-treatment with Isoliensinine failed to attenuate apoptosis in the Si-PI3K or Si-AKT groups, suggesting that the anti-apoptotic effects of Isoliensinine depend on the integrity of PI3K/AKT pathway. These results provided functional evidence supporting PI3K and AKT as critical mediators of Isoliensinine protective effects against cardiomyocyte apoptosis.

4. Discussion

Hypertension-induced cardiac apoptosis plays a critical role in the progression of cardiovascular diseases, underscoring the urgent need for therapeutic strategies targeting this pathological process[28]. A previous study has demonstrated that Isoliensinine, a natural isoquinoline alkaloid, possesses significant antihypertensive properties[24]. In the present study, we further revealed that Isoliensinine alleviates cardiac dysfunction, structural remodeling, and cardiomyocyte apoptosis in SHR and AngII-stimulated H9c2 cells. These cardioprotective effects are primarily mediated through modulation of the PI3K/AKT signaling pathway, providing new mechanistic insights and potential therapeutic value in the treatment of hypertension-induced cardiac injury.

Chronic hypertension imposes sustained pressure overload on the left ventricle, resulting in compensatory hypertrophy, as reflected by an elevated IVS;d. Prolonged elevation in afterload progressively impairs myocardial contractility, leading to reductions in LVEF and LVFS[29]. This decline in systolic performance causes end-diastolic volume accumulation and chamber dilation, as evidenced by increased LVID;d[30]. Eventually, these maladaptive changes are accompanied by interstitial fibrosis and myofiber disarray, hallmark features of pathological cardiac remodeling and functional deterioration [31]. In our study for the first time, Isoliensinine significantly improved LVEF and LVFS, while reducing IVS;d and LVID;d in SHRs. Furthermore, histological analysis revealed marked attenuation of myocardial structural disorganization, highlighting Isoliensinine's efficacy in attenuating hypertension-induced cardiac remodeling. Nevertheless, we acknowledge the limitations of this study, including a relatively small sample size and reliance on a single animal model (SHR). Future studies should incorporate larger sample sizes and alternative models, such as AngII-induced or salt-sensitive hypertension models, to enhance translational relevance. Clinical validation in human-derived samples is also warranted to confirm Isoliensinine's therapeutic potential.

Apoptosis of cardiomyocyte s is a key pathological feature in hypertension-induced cardiac injury[32]. Given the terminally differentiated nature of cardiomyocytes and their limited regenerative capacity, their loss has profound consequences[33]. During the progression of hypertension-induced cardiac injury, excessive mechanical stress and aberrant activation of AngII, a central effector of the

renin-angiotensin-aldosterone system, is known to exacerbate apoptosis via oxidative stress and inflammatory signaling under hypertensive conditions [34, 35], ultimately leading to irreversible cardiac remodeling and dysfunction [36]. In our study, bioinformatic analysis revealed that apoptosis-related pathways are significantly affected by Isoliensinine. We confirmed its anti-apoptotic effects both *in vivo* and *in vitro*, evidenced by a reduced apoptotic index in cardiac tissue of SHR and inhibition of AngII-induced apoptosis in H9C2 cells. Western blotting further showed downregulation of the pro-apoptotic protein Bax and upregulation of the anti-apoptotic protein Bcl-2, alongside suppression of cleaved caspase-3.

The PI3K/AKT signaling pathway is a well-established mediator of anti-apoptotic mechanisms[37, 38]. Phosphorylated AKT promotes cell survival by inhibiting Bax activation and downstream caspase-3 cleavage [39]. Our mechanistic investigations revealed that Isoliensinine significantly restored PI3K/AKT pathway activity, and the use of a pathway activator further supported that the anti-apoptotic effects of Isoliensinine are largely dependent on this signaling axis. Although the current study focused on PI3K/AKT signaling, RNA sequencing analysis also highlighted the enrichment of other relevant pathways, including HIF-1 and mTOR, which may contribute to the observed effects. These pathways remain unexplored in this study and warrant further investigation in future work.

Recent studies have indicated that UCL-TRO-1938 interacts with p85 regulatory and the catalytic subunit p110α of PI3Kα, relieve autoinhibition and enhance kinase activity[40, 41]. Similarly, the pleckstrin homology (PH) domain of AKT1 (amino acids 1–106 at the N-terminus) specifically binds to phosphatidylinositol (3,4,5)-trisphosphate (PIP3), facilitating membrane translocation and activation [42]. In this study, molecular docking simulations indicated strong binding affinity of Isoliensinine to PI3K and AKT. These in silico findings were further validated experimentally by CESTA and Western blotting, suggesting a potential direct interaction. However, the precise binding sites and nature of the interaction remains to be elucidated. Future studies employing advanced biophysical methods such as surface plasmon resonance (SPR) or biolayer interferometry (BLI), along with structural modeling or crystallography, are essential for confirming these interactions and define the precise molecular mechanisms underlying the cardioprotective effects of Isoliensinine.

Our findings provide novel evidence supporting that Isoliensinine as a promising therapeutic candidate for hypertension-induced cardiac injury. By targeting the PI3K/AKT signaling pathway and inhibiting cardiomyocyte apoptosis, Isoliensinine holds potential for the development of new interventions to prevent or treat hypertensive cardiac damage.

5. Conclusion

Isoliensinine alleviates cardiomyocyte apoptosis in SHR and AngII-stimulated H9C2 cells, primarily through the restoration of PI3K/AKT pathway activity and modulation of multiple related signaling pathways (see Graphical abstract). These findings offer novel insights into the therapeutic potential of Isoliensinine for hypertensive cardiomyopathy and highlight its promise as a candidate for future clinical application.

Funding

This research was funded by National Natural Science Foundation of China, grant number U22A20372, 82204662; Development Fund of Chen Keji Integrative Medicine, grant number CKJ2022017; The youth talent support program from Fujian University of Traditional Chinese Medicine, Fujian Research and Training Grants for Young and Mid-dle-aged Leaders in Healthcare, grant number XQB202202; Fujian Province Young and Mid-dle-aged Teacher Education Research Project (Science and Technology), grant number JZ240026; School management project of Fujian University of Traditional Chinese Medicine, grant number X2024008; Fujian Natural Science Foundation for Distinguished Young Scholars, grant number 2024J010032.

Data Availability Statement

The data used to support the findings of this study are available from the corresponding author upon request. The RNA sequencing data used in this study are stored in the NCBI Gene Expression Omnibus with the registration number GSE281553.

Conflict of interest statement

There are no conflicts of interest.

Reference

[1] Abissegue G., Yakubu S. I., Ajay A. S., et al, A systematic review of the epidemiology and the public health implications of stroke in Sub-Saharan Africa, J Stroke Cerebrovasc Dis. 33 (2024) 107733. https://doi.org/10.1016/j.jstrokecerebrovasdis.2024.107733.

[2] Manolis A. A., Manolis T. A., Manolis A. S., Current Strategies for Atrial Fibrillation Prevention and Management: Taming the Commonest Cardiac Arrhythmia, Curr Vasc Pharmacol. (2024) https://doi.org/10.2174/0115701611317504240910113003.

[3] Perrotta S., Carnevale L., Perrotta M., et al, A heart-brain-spleen axis controls cardiac remodeling to hypertensive stress, Immunity. 58 (2025) 648-665 e647. https://doi.org/10.1016/j.immuni.2025.02.013.

[4] Ye S., Huang H. A.-O., Han X., et al, Dectin-1 Acts as a Non-Classical Receptor of Ang II to Induce Cardiac Remodeling, Circ Res. 17 (2023) 707-722. https://doi.org/10.1161/CIRCRESAHA.

[5] Roudi H. S., Safaei R., Dabbaghi M. M., et al, Mechanistic Insights on Cardioprotective Properties of Ursolic Acid: Regulation of Mitochondrial and Non-mitochondrial Pathways, Curr Pharm Des. (2024) https://doi.org/10.2174/0113816128344497241120025757.

[6] Yan T., Yu H., Li T., et al, Mechanisms of Cardiovascular Toxicities Induced by Cancer Therapies and Promising Biomarkers for Their Prediction: A Scoping Review, Heart Lung Circ. 33 (2024) 605-638. https://doi.org/10.1016/j.hlc.2023.12.006.

[7] Carneiro B. A., El-Deiry W. S., Targeting apoptosis in cancer therapy, Nat Rev Clin Oncol. 17 (2020) 395-417. https://doi.org/10.1038/s41571-020-0341-y.

[8] Qi B., He L., Zhao Y., et al, Akap1 deficiency exacerbates diabetic cardiomyopathy in mice by NDUFS1-mediated mitochondrial dysfunction and apoptosis, Diabetologia. 63 (2020) 1072-1087. https://doi.org/10.1007/s00125-020-05103-w.

[9] Feng R., Wang D., Li T., et al, Elevated SLC40A1 impairs cardiac function and exacerbates mitochondrial dysfunction, oxidative stress, and apoptosis in ischemic myocardia, Int J Biol Sci. 20 (2024) 414-432. https://doi.org/10.7150/ijbs.89368.

[10] Wang Q., Yang X., Song Y., et al, Astragaloside IV-targeting miRNA-1 attenuates lipopolysaccharide-induced cardiac dysfunction in rats through inhibition of apoptosis and autophagy, Life Sci. 275 (2021) 119414. https://doi.org/10.1016/j.lfs.2021.119414.

[11] Mustafa M., Ahmad R., Tantry I. Q., et al, Apoptosis: A Comprehensive Overview of Signaling Pathways, Morphological Changes, and Physiological Significance and Therapeutic Implications, Cells. 13 (2024) https://doi.org/10.3390/cells13221838.

[12] Zhang F., Guo Z., Wu M., et al, Trifolin attenuates hypertension-mediated cardiac injury by inhibiting cardiomyocyte apoptosis: Mechanistic insights and therapeutic potential, Eur J Pharmacol. 985 (2024) 177125. https://doi.org/10.1016/j.ejphar.2024.177125.

[13] Christidi E., Brunham L. R., Regulated cell death pathways in doxorubicin-induced cardiotoxicity, Cell Death Dis. 12 (2021) 339. https://doi.org/10.1038/s41419-021-03614-x.

[14] Chen H., Chen C., Spanos M., et al, Exercise training maintains cardiovascular health: signaling pathways involved and potential therapeutics, Signal Transduct Target Ther. 7 (2022) 306. https://doi.org/10.1038/s41392-022-01153-1.

[15] Osborne B., Patel R. S., Krause-Hauch M., et al, Small Molecule Inhibitor of Protein Kinase C DeltaI (PKCdeltaI) Decreases Inflammatory Pathways and Gene Expression and Improves Metabolic Function in Diet-Induced Obese Mouse Model, Biology (Basel). 13 (2024) https://doi.org/10.3390/biology13110943.

[16] Liu Z.-H., Yu B.-B., Zhou H.-H., et al, Characteristic components from Rehmannia radix and their effects on insulin resistance through PI-3K/AKT signaling pathway in HepG2 Cells, Food & Medicine Homology. (2025) https://doi.org/10.26599/fmh.2025.9420073.

[17] Zhang T., Li L., Mo X., et al, Matairesinol blunts adverse cardiac remodeling and heart failure induced by pressure overload by regulating Prdx1 and PI3K/AKT/FOXO1 signaling, Phytomedicine. 135 (2024) 156054. https://doi.org/10.1016/j.phymed.2024.156054.

[18] Dong J., Zhang B.-D., Li S., et al, Identification of sesquiterpenes from Curcuma longa and its potential for alcoholic liver disease based on FBMN strategy and network pharmacology, Food & Medicine Homology. (2025) https://doi.org/10.26599/fmh.2026.9420114.

[19] Zhao L., Cao H., Yuan Y., et al, Annexin A5 knockdown inhibits cardiomyocyte apoptosis and alleviates cardiac hypertrophy via activating the PI3K/AKT/Bcl-2 signaling pathway, Sci Rep. 14 (2024) 31915. https://doi.org/10.1038/s41598-024-83244-3.

[20] Chen L., Chen L. J., Shen H. W., et al, Inhibition of HIF-2alpha expression in cardiomyocytes attenuates PCB126-induced cardiotoxicity associated with decreased apoptosis through the PI3K/Akt and p53 signaling pathways, Ecotoxicol Environ Saf. 286 (2024) 117185. https://doi.org/10.1016/j.ecoenv.2024.117185.

[21] Tuzimski T., Petruczynik A., New trends in the practical use of isoquinoline alkaloids as potential drugs applicated in infectious and non-infectious diseases, Biomed Pharmacother. 168 (2023) 115704. https://doi.org/10.1016/j.biopha.2023.115704.

[22] Zhang C., Deng J., Liu D., et al, Nuciferine ameliorates hepatic steatosis in high-fat diet/streptozocin-induced diabetic mice through a PPARalpha/PPARgamma coactivator-1alpha pathway, Br J Pharmacol. 175 (2018) 4218-4228. https://doi.org/10.1111/bph.14482.

[23] Bishayee A., Patel P. A., Sharma P., et al, Lotus (Nelumbo nucifera Gaertn.) and Its Bioactive Phytocompounds: A Tribute to Cancer Prevention and Intervention, Cancers (Basel). 14 (2022) https://doi.org/10.3390/cancers14030529.

[24] Yao M., Wu M., Yuan M., et al, Enhancing the therapeutic potential of isoliensinine for hypertension through PEG-PLGA nanoparticle delivery: A comprehensive in vivo and in vitro study, Biomed Pharmacother. 174 (2024) 116541. https://doi.org/10.1016/j.biopha.2024.116541.

[25] Cai Q., Zhao C., Xu Y., et al, Qingda granule alleviates cerebral ischemia/reperfusion injury by inhibiting TLR4/NF-κB/NLRP3 signaling in microglia, J Ethnopharmacol. 24 (2024) 324:117712. https://doi.org/10.1016/j.jep.2024.117712.

[26] Rajadnya R., Sharma N., Mahajan A., et al, Novel systems biology experimental pipeline reveals matairesinol's antimetastatic potential in prostate cancer: an integrated approach of network pharmacology, bioinformatics, and experimental validation, Brief Bioinform. 25 (2024) https://doi.org/10.1093/bib/bbae466.

[27] Luo P., Zhang Q., Zhong T. Y., et al, Celastrol mitigates inflammation in sepsis by inhibiting the PKM2-dependent Warburg effect, Mil Med Res. 9 (2022) 22. https://doi.org/10.1186/s40779-022-00381-4.

[28] Al-Hasani J., Sens-Albert C., Ghosh S., et al, Zyxin protects from hypertension-induced cardiac dysfunction, Cell Mol Life Sci. 79 (2022) 93. https://doi.org/10.1007/s00018-022-04133-4.

[29] Yuan P., Liu J., Xiong S., et al, Effects and mechanism of Compound Qidan Formula on rats with HFpEF induced by hypertension and diabetes mellitus based on Ang II/TGF-β1/Smads signaling pathway, J Ethnopharmacol. 15 (2023) 313:116558. https://doi.org/10.1016/j.jep.2023.116558.

[30] Feng X., Yan M., Tang L., et al, Effects of intensive blood-pressure treatment on myocardial work in elderly hypertensive patients: A subcenter study of the STEP randomized controlled trial, Clin Cardiol. 47 (2024) e24172. https://doi.org/10.1002/clc.24172.

[31] Zhang Y. L., Bai J., Yu W. J., et al, CD11b mediates hypertensive cardiac remodeling by regulating macrophage infiltration and polarization, J Adv Res. 55 (2024) 17-31. https://doi.org/10.1016/j.jare.2023.02.010.

[32] Xue F., Cheng J., Liu Y., et al, Cardiomyocyte-specific knockout of ADAM17 ameliorates left ventricular remodeling and function in diabetic cardiomyopathy of mice, Signal Transduct Target Ther. 7 (2022) 259. https://doi.org/10.1038/s41392-022-01054-3.

[33] Hinton A., Jr., Claypool S. M., Neikirk K., et al, Mitochondrial Structure and Function in Human Heart Failure, Circ Res. 135 (2024) 372-396. https://doi.org/10.1161/CIRCRESAHA.124.323800.

[34] de la Fuente-Muñoz M., Román-Carmena M. A.-O., Amor S. A.-O., et al, Supplementation with the Postbiotic BPL1™-HT (Heat-Inactivated Bifidobacterium animalis subsp. Lactis) Attenuates the Cardiovascular Alterations Induced by Angiotensin II Infusion in Mice. Antioxidants (Basel). 8 (2025) 193. https://doi.org/10.3390/antiox14020193.

[35] Xiao D., Lu T., Jiang M., et al, Natural active ingredient identification from food and medicine homology products Achyranthis bidentatae radix and Saururus chinensis in hypertrophic cardiomyopathy and hypertension by bioinformatics and CADD approaches, Food & Medicine Homology. (2025) https://doi.org/10.26599/fmh.2026.9420103.

[36] Zhang F., Guo Z., Wu M., et al, Trifolin attenuates hypertension-mediated cardiac injury by inhibiting cardiomyocyte apoptosis: Mechanistic insights and therapeutic potential, Eur J Pharmacol. 985 (2024) 177125. https://doi.org/10.1016/j.ejphar.2024.177125.

[37] Li G.-R., Xia G.-Y., Zhou L.-N., et al, Albiflorin: a promising natural monoterpene glycoside with potential therapeutic benefits for multiple physiological systems, Food & Medicine Homology. (2024) https://doi.org/10.26599/fmh.2025.9420064.

[38] Liang H., Guan M., Li T., et al, Critical review on biological effect and mechanisms of diterpenoids in Rosmarinus officinalis, Food & Medicine Homology. (2025) https://doi.org/10.26599/fmh.2025.9420021.

[39] Chen L., Chen L. J., Shen H. W., et al, Inhibition of HIF-2α expression in cardiomyocytes attenuates PCB126-induced cardiotoxicity associated with decreased apoptosis through the PI3K/Akt and p53 signaling pathways, Ecotoxicol Environ Saf. 1 (2024) 286:117185. https://doi.org/10.1016/j.ecoenv.2024.117185.

[40] Gong G. A.-O., Bilanges B. A.-O., Allsop B., et al, A small-molecule PI3Kα activator for cardioprotection and neuroregeneration, Nature. 618 (2025) 159-168. https://doi.org/10.1038/s41586-023-05972-2.

[41] Golforoush P., Sulaiman E., He D., et al, An activator of PI3Kα restores cardioprotection from ischaemia/reperfusion injury in mice with coronary atherosclerosis or insulin resistance. Cardiovasc Res. 13 (2025) cvaf111. https://doi.org/10.1093/cvr/cvaf111.

[42] Yin S., Liu L., Brobbey C., et al, PRMT5-mediated arginine methylation activates AKT kinase to govern tumorigenesis, Nat Commun. 12 (2021) 3444. https://doi.org/10.1038/s41467-021-23833-2.